

# Bang-Bang Charging of Electrical Vehicles by Smart Grid Technology

Y. Shi, H. D. Tuan, T. Q. Duong, H. V. Poor and A. V. Savkin,

## Abstract

The success of the transportation electrification in this century particularly requires the penetration of the internet of plug-in electric vehicles (PEVs) into the smart power grid. Beside the function of serving the traditional residential power demand, next-generation power grids also aim to support the internet of PEVs at the same time. The distinct difference between the traditional power demand and PEVs' power demand is that while the statistics of the former is rich enough for treating it as inelastic/known before hand, the latter is unknown until random PEVs' arrivals. Massive penetration of PEVs certainly causes the grid unpredictable fluctuation. The present paper considers the joint PEVs charging coordination and grid power generation to minimizing both of the negative impact of PEVs' integration and the cost of power generation while meeting the grid operating constraints and all parties' demand. The bang-bang PEVs charging strategy is adopted to exploit its simple implementation. By using a recently developed model predictive control (MPC) model for this problem, the online computation is based on a predictive mixed integer nonlinear programming (MINP). A new solution computation for this optimization problem is developed. Its capacity of achieving the globally optimal solution is shown by numerical comparison between its performance and that by an off-line optimal solution.

## Index Terms

Smart power grid, plug-in electric vehicles (PEVs), model predictive control (MPC), bang-bang control, mixed integer nonlinear programming, mixed integer convex programming.

Ye Shi and Hoang D. Tuan are with the School of Electrical and Data Engineering, University of Technology Sydney, Broadway, NSW 2007, Australia (email: Ye.Shi@student.uts.edu.au, Tuan.Hoang@uts.edu.au)

Trung Q. Duong is with Queen's University Belfast, Belfast BT7 1NN, UK (email: trung.q.duong@qub.ac.uk)

H. Vincent Poor is with the Department of Electrical Engineering, Princeton University, Princeton, NJ 08544, USA (e-mail: poor@princeton.edu)

Andrey V. Savkin with the School of Electrical Engineering and Telecommunications, The University of New South Wales Sydney, NSW 2052, Australia (email: a.savkin@unsw.edu.au)

## I. INTRODUCTION

Due to the increasing awareness of energy consumption and environment pollution from traditional fossil fuel, as well as the development of battery and charging technology, there will be a significant growing number of plug-in electric vehicles (PEVs) within the next few years [1]. The PEVs will play an important role in the future smart grid because of the benefits such as, lower operation cost, less air pollution emissions and better utilization of renewable energy [2]. However, as most PEVs utilize grid power for charging, the growing penetration of PEV could pose potential threats to the existing smart grid. Unregulated charging of PEV may lead to serious overloading, additional power loss and unacceptable voltage violation in smart grid system [3], [4]. Therefore, optimal scheduling for PEV charging aims at minimizing the total cost of PEVs and smart grid, while satisfying the charging demand of PEV and operation constraints of smart grid is necessary to study.

Recently, various works have addressed the optimal scheduling problem for PEVs in smart grid [5]–[8]. A mixed integer linear programming (MILP) formulation was proposed in [9] to optimize the daily cost on PEV charging involving with linear dc power flow constraint. The disadvantage of dc power flow is clearly especially in smart grid, due to the higher dc error and exclusion of bus voltage and reactive power from the model. Reference [6] proposed a mixed integer nonlinear programming (MINLP) model for optimal scheduling of PEV in an unbalanced distributed system. The MINLP problem was then linearized to MILP problem by some linearization techniques such as the first order Taylor expansion and piecewise linear approximation. As a result, its solution of MILP is not necessarily feasible to the original MINLP problem. In [7], a similar MILP model with [6] was proposed by adding a vehicle-to-grid (V2G) charging strategy, which allows PEV behaving as bidirectional power source to reduce the negative effect at peak time [5]. However, [10] raised concern about the cost and techniques for discharging of PEV. In addition, the above reference for PEV charging all applied static scheduling strategy, which assumed that information including PEV arrival time, departure time and initial SOC are given beforehand. However, it is not realistic to obtain all of those information in advance.

Model predictive control (MPC) approach for dynamic PEV scheduling has emerged as a promising solution to deal with the system dynamic and uncertainty. In [11], a MPC-based model was formulated to schedule PEV charging in a finite horizon, but the operation constraints of grid

were not considered. Additionally, its assumption of PEV could be fully charged in only one time slot is unrealistic due to the physical limitation of PEV itself. A MILP model formulated over a rolling horizon window for energy storage control was proposed in [12], while the voltage balance was ignored. [13] presented a MILP-based MPC for integrated PEVs scheduling in microgrid. Three-types of PEV charging scenarios are provided, including bidirectional, unidirectional and one block charging. However, the stochastic optimization in [13] suffers from large computational cost.

In this paper, both the dynamic and static scheduling for PEV charging are studied. A novel MPC-based two-stage computational solution is proposed to iteratively solve the dynamic scheduling problem. The static scheduling scenario serves as a counterpart to investigate the optimality of the MPC-based solution of dynamic scenario. Extensive simulation results based on real electricity price and residential demand shows that the proposed method is effective and practical.

The rest of the paper is structured as follows. Section II is devoted to the problem statement of the PEV charging scheduling problem, which is formulated as a MINLP model in section III. A dynamic computational solution for dynamic scheduling scenario, using the proposed MPC-based two-stage approach is developed in Section IV. A static computational solution for static scheduling scenario is considered in Section V. Section VI provides the computational results and Section VI concludes the paper.

*Notation.* The notation used in this paper is standard. Particularly,  $j$  is the imaginary unit,  $X^H$  is Hermitian transpose of a vector/matrix  $X$ ,  $M \succeq 0$  for a Hermitian symmetric matrix  $M$  means that it is positive semi-definite,  $\text{rank}(M)$  and  $\text{Trace}(M)$  are the rank and trace of a matrix  $M$ , respectively.  $\Re(\cdot)$  and  $\Im(\cdot)$  are the real and imaginary parts of a complex quantity, and  $a \leq b$  for two complex numbers  $a$  and  $b$  is componentwise understood, i.e.  $\Re(a) \leq \Re(b)$  and  $\Im(a) \leq \Im(b)$ . The cardinality of a set  $\mathcal{C}$  is denoted by  $|\mathcal{C}|$ .  $\lceil x \rceil$  is the smallest integer that is not less than  $x$ .

## II. PROBLEM STATEMENT

We consider a joint problem of PEV charging scheduling and power control in an residential grid, which aims at saving operation costs for both PEVs and power generation, with demands of PEVs charging and residential power grid satisfied. In the power grid, active and reactive power balance between supply and demand, physical limitations of grid including voltage and power

bounds are taken into account. The serving time period of the grid is divided into  $T$  time slots  $\mathcal{T} := \{1, 2, \dots, T\}$ . Each time slot has a time duration  $\delta_t$ , which usually varies from 30 minutes to an hour. In addition, price-inelastic load varies from each time interval  $[t, t + 1]$  according to the residential specification. In this paper, the following are assumed:

- The SOC of each PEV is known after plugged into the grid, and it must be fully charged by departure during the charging period  $\mathcal{T}$ ;
- The charging of PEV must be operated in a given period of time slots, Fig.1 illustrates the charging period of a PEV;
- The PEVs can communicate with the grid and update the information of charging state, which can be controlled in each time interval during the charging period  $\mathcal{T}$ .

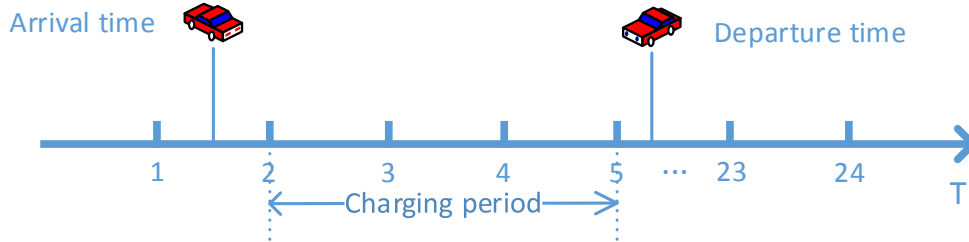


Fig. 1: Illustration of the charging period of a PEV

Charging demands specified by charging tasks of PEVs and grid demands including active and reactive power balance between demand and supply, voltage and power limitations must be satisfied. In addition, we consider the objective as minimizing the total cost of PEVs charging and active power generation among the whole charging period  $\mathcal{T}$ . The charging state of a PEV can be represented by a binary variable  $\tau \in \{0, 1\}$ .  $\tau = 1$  denotes the battery is charging at a fixed rate, while  $\tau = 0$  denotes the battery is not charging.

In this paper, both static and dynamic scheduling of PEV charging are studied. In the static charging scenario, all the information including PEV arrival time, departure time and initial SOC are given beforehand. The grid utility optimizes the variables of charging rate and active power by an algorithm and then all PEVs will follow the scheduling profile after plugged into the grid. However, it is not realistic to obtain all of those charging information in advance. Additionally, it is also not possible to have a stable long-term scheduling profile for the grid. Therefore, to

tackle the PEV charging problem more realistic, it is significant to adopt the dynamic charging scenario, in which the utility calculates the optimal charging scheduling only for PEVs that connected with the grid at the current time slot. In the next time slot, the utility will update the charging information such as the set of PEVs connected in the grid, the SOC of PEVs and re-do the calculation. The above dynamic procedure is the basic idea of MPC approach. We will focus on the dynamic charging scenario in this work, and the static scenario will serve as a counterpart to investigate the optimality of our MPC-based dynamic charging method.

### III. MINLP MODEL FORMULATION

The joint problem of PEV charging scheduling and power control in an residential grid can be formulated as a MINLP problem. Consider a residential power grid with a set of buses  $\mathcal{N} := \{1, 2, \dots, N\}$  connected through a set of flow lines  $\mathcal{L} \subseteq \mathcal{N} \times \mathcal{N}$ , i.e. bus  $k$  is connected to bus  $m$  if and only if  $(k, m) \in \mathcal{L}$ . Accordingly,  $\mathcal{N}(k)$  is the set of other buses connected to bus  $k$ . There is a subset  $\mathcal{G} \subseteq \mathcal{N}$ , whose elements are connected to distributed generators (DGs). Any bus  $k \in \mathcal{N} \setminus \mathcal{G}$  is thus not connected to DGs. Any bus  $k \in \mathcal{G}$  also has a function to serve PEVs and in what follow is also referred to CS  $k$ . By defining  $M = |\mathcal{G}|$ , there are  $M$  CSs in the grid. Denote by  $\mathcal{H}_k$  the set of those PEVs that arrive at CS  $k$ . Accordingly,  $k_n$  is the  $n$ -th PEV that arrives at CS  $k$ . Following is a description of the MINLP model formulation, including constraints and objective function.

#### A. Constraints of PEV Charging

PEV  $k_n$  arrives at  $t_{a,k_n} \in \mathcal{T}$  and needs to depart by  $t_{k_n,d} \in \mathcal{T}$ . The constraint

$$t_{k_n,d} - t_{k_n,a} \leq T_{k_n}, \quad (1)$$

expresses the PEV  $k_n$ 's time demand.

Suppose that  $C_{k_n}$  and  $s_{k_n}^0$  are the battery capacity and initial SOC of PEV  $k_n$ . It must be fully charged by the departure time  $t_{k_n,d}$ , i.e.

$$\sum_{t'=t_{k_n,a}}^{t_{k_n,d}} u_h \bar{P}_{k_n} \tau_{k_n}(t') \geq C_{k_n} (1 - s_{k_n}^0), \quad (2)$$

where  $u_h$  is the charging efficiency of the battery,  $\bar{P}_{k_n}(t')$  is fix charging rate of PEV  $k_n \in \mathcal{H}_k$ ,  $\tau_{k_n}(t')$  denotes the binary variables to represent the charging state of PEV  $k_n \in \mathcal{H}_k$ ,

$$\tau_{k_n}(t') = \begin{cases} 1, & \text{If PEV } k_n \text{ is charging at time } t'; \\ 0, & \text{If PEV } k_n \text{ is not charging at time } t'. \end{cases} \quad (3)$$

For ease of presentation, if  $t' \notin [t_{k_n,a}, t_{k_n,b}]$  we set  $\tau_{k_n}(t') = 0$ .

### B. Constraints of Grid Limitations

The next constraints relate to the acceptable range of generated power by the DGs:

$$\underline{P}_{g_k} \leq P_{g_k}(t') \leq \overline{P}_{g_k}, \quad k \in \mathcal{G}, \quad (4)$$

and

$$\underline{Q}_{g_k} \leq Q_{g_k}(t') \leq \overline{Q}_{g_k}, \quad k \in \mathcal{G}, \quad (5)$$

where  $\underline{P}_{g_k}$ ,  $\underline{Q}_{g_k}$  and  $\overline{P}_{g_k}$ ,  $\overline{Q}_{g_k}$  are respectively the lower and upper limit of the real generated and reactive generated powers,  $P_{g_k}(t')$  and  $Q_{g_k}(t')$  are the real and reactive powers generated by DG  $k$ , respectively.

The constraints of voltage are

$$\underline{V}_k \leq |V_k(t')| \leq \overline{V}_k, \quad k \in \mathcal{N}, \quad (6)$$

$$|\arg(V_k(t')) - \arg(V_m(t'))| \leq \theta_{km}^{\max}, \quad (k, m) \in \mathcal{L}, t' \in \mathcal{T}, \quad (7)$$

where  $\underline{V}_k$  and  $\overline{V}_k$  are the lower limit and upper limit of the voltage amplitude, while  $\theta_{k,m}^{\max}$  are given to express the voltage phase balance.

### C. Constraints of PEV & Power Balance

Followed by [14], for  $k \in \mathcal{G}$ , the total supply and demand energy is balanced as

$$\begin{aligned} V_k(t') \left( \sum_{m \in \mathcal{N}(k)} y_{km} (V_k - V_m) \right)^* &= (P_{g_k}(t') - P_{l_k}(t')) \\ &- \sum_{n \in \mathcal{H}_k} \overline{P}_{k_n} \tau_{k_n}(t') + j(Q_{g_k}(t') - Q_{l_k}(t')), \quad k \in \mathcal{G}, \end{aligned} \quad (8)$$

for  $k \in \mathcal{N} \setminus \mathcal{G}$ ,

$$\begin{aligned} V_k(t) \left( \sum_{m \in \mathcal{N}(k)} y_{km} (V_k - V_m) \right)^* &= \\ &-P_{l_k}(t') - jQ_{l_k}(t'), \quad k \in \mathcal{N} \setminus \mathcal{G}, \end{aligned} \quad (9)$$

where  $y_{km} \in \mathbb{C}$  is the admittance of line  $(k, m)$  and  $P_{l_k}(t')$  and  $Q_{l_k}(t')$  are respectively known real and reactive price-inelastic demands at bus  $k$  to express the residential power demand

The problem of interest is to minimize both the energy cost to DGs and charging cost for PEVs. Thus, by defining

$$\begin{aligned} V(t') &= (V_1(t'), \dots, V_N(t')), \mathcal{V} = \{V(t')\}_{t' \in \mathcal{T}}, \\ P_g(t') &= (P_{g_1}(t'), \dots, P_{g_M}(t')), \\ Q_g(t') &= (Q_{g_1}(t'), \dots, Q_{g_M}(t')), \\ R(t') &= \{P_g(t'), Q_g(t')\}, \mathcal{R} = \{R(t')\}_{t' \in \mathcal{T}}, \end{aligned}$$

and

$$\begin{aligned} \mathcal{P}^{PEV} &= \{\tau^{PEV}(t')\}_{t' \in \mathcal{T}}, \\ \tau^{PEV}(t') &= \{\tau_{k_n}(t')\}_{k_n \in \mathcal{H}_k, k=1, \dots, M}, \end{aligned}$$

the objective function is given by

$$F(\mathcal{R}, \mathcal{P}^{PEV}) = \sum_{t' \in \mathcal{T}} \sum_{k \in \mathcal{G}} f(P_{g_k}(t')) + \sum_{t' \in \mathcal{T}} \sum_{k \in \mathcal{N}} \sum_{n \in \mathcal{H}_k} \beta_t \bar{P}_{k_n} \tau_{k_n}(t') \quad (10)$$

where  $f(P_{g_k}(t'))$  is the cost function of real power generation by DGs, which is linear or quadratic in  $P_{g_k}(t')$ , and  $\beta_t$  is the known PEV charging price during the time interval  $(t', t' + 1]$ .

The joint PEV charging scheduling and voltage control is mathematically formulated as

$$\min_{\mathcal{V}, \mathcal{R}, \mathcal{P}^{PEV}} F(\mathcal{R}, \mathcal{P}^{PEV}) \quad \text{s.t.} \quad (2) - (9) \quad (11)$$

The above problem (11) is MINLP, which is nonconvex and very computationally challenging because of the quadratic equality constraints (8) and (9), nonlinear inequality constraints (6) and (7) and integer constraints (3). Moreover, the arrival time  $t_{k_n, a}$  of each individual PEV  $k_n$ , its charging demand and its departure time  $t_{k_n, d}$  are unknown. Generally, linearization techniques such as first order Taylor expansion and piece wise approximation are applied to handle the nonlinear constraints (8), (9), (6) and (7) in the above MINLP problem [6], [7], [9]. After the linearization, MILP model is obtained, which can be efficiently solved under the framework of commercial solver CPLEX. However, the found result are not necessarily feasible to the original problem (11) because the linearization techniques can not guarantee the consistence between the MINLP and MILP. In the next section, a novel MPC-based two-stage computational solution will be proposed to iteratively solve the MINLP problem (11).

#### IV. MPC-BASED TWO-STAGE COMPUTATIONAL SOLUTION FOR DYNAMIC SCHEDULING

Considering  $(R(t'), P^{PEV}(t'))$  and  $V(t')$  as the plant state and control, respectively, equations (4), (5), (8) and (9) provide state behavioral equations [15] with the end constraint (2) together with (2), while equations (6) and (7) provide control constraints. On the surface, (11) appears to be a control problem over the finite horizon  $[1, T]$ . However, all equations in (11) are unpredictable beforehand, preventing the application of conventional model predictive control [16], [17]. We now follow the idea of [18] to address (11).

At each time  $t$  denote by  $C(t)$  the set of PEVs that need to be charged. For each  $k_n \in C(t)$ , let  $\mathcal{P}_{k_n}(t)$  be its remaining demand for charging by the departure time  $t_{k_n,d}$ . Define

$$\Psi(t) = \max_{k_n \in C(t)} t_{k_n,d}. \quad (12)$$

At time  $t$  we solve the following MINLP problem over the prediction horizon  $[t, \Psi(t)]$  but then take only  $V(t), P_{k_n}(t), R(t)$  for online updating solution of (11):

$$\min_{V(t'), R(t'), \tau_{k_n}(t'), t' \in [t, \Psi(t)], k_n \in C(t)} F_{[t, \Psi(t)]} \quad (13a)$$

$$\text{s.t. (4) - (7), (9), for } t' \in [t, \Psi(t)], \quad (13b)$$

$$\begin{aligned} & V_k(t') \left( \sum_{m \in \mathcal{N}(k)} y_{km} (V_k(t') - V_m(t')) \right)^* = \\ & (P_{g_k}(t') - P_{l_k}(t') - \sum_{k_n \in C(t)} \bar{P}_{k_n} \tau_{k_n}(t')) \\ & + j(Q_{g_k}(t') - Q_{l_k}(t')), \quad (t', k) \in [t, \Psi(t)] \times \mathcal{G}, \end{aligned} \quad (13c)$$

$$\sum_{t'=t}^{t_{k_n,d}} u_h \bar{P}_{k_n} \tau_{k_n}(t') \geq \mathcal{P}_{k_n}(t), t' \in [t, \Psi(t)], \quad (13d)$$

$$\tau_{k_n}(t') \in \{0, 1\}, t' \in [t, \Psi(t)], \quad (13e)$$

with  $F_{[t, \Psi(t)]} := \sum_{t'=t}^{\Psi(t)} \sum_{k \in \mathcal{G}} f(P_{g_k}(t')) + \sum_{t'=t}^{\Psi(t)} \sum_{k_n \in C(t)} \beta_t \bar{P}_{k_n} \tau_{k_n}(t')$ . One can notice that (13) includes only what is known at the present time  $t$ . Of course, (13) is still a difficult MINLP and in the end we need only its solution at  $t$ , so we propose the following approach in tackling its solution at  $t$ .

Define the Hermitian symmetric matrix  $W(t') = V(t')V^H(t') \in \mathbb{C}^{N \times N}$ , which must satisfy  $W(t') \succeq 0$  and  $\text{rank}(W(t')) = 1$ . By replacing  $W_{km}(t') = V_k(t')V_m^*(t')$ ,  $(k, m) \in \mathcal{N} \times \mathcal{N}$  in, we

reformulate (13) to the following optimization problem in matrices  $W(t') \in \mathbb{C}^{N \times N}$ ,  $t' \in [t, \Psi(t)]$ :

$$\min_{W(t'), R(t'), \tau_{k_n}(t'), t' \in [t, \Psi(t)], k_n \in C(t)} F_{[t, \Psi(t)]} \quad (14a)$$

$$\text{s.t. (4) - (5), for } t' \in [t, \Psi(t)], \quad (14b)$$

$$\begin{aligned} & \sum_{m \in \mathcal{N}(k)} (W_{kk}(t') - W_{km}(t')) y_{km}^* = (P_{g_k}(t') - P_{l_k}(t') \\ & - \sum_{k_n \in C(t)} \bar{P}_{k_n} \tau_{k_n}(t')) + j(Q_{g_k}(t') - Q_{l_k}(t')), \quad k \in \mathcal{G}, \end{aligned} \quad (14c)$$

$$\begin{aligned} & \sum_{m \in \mathcal{N}(k)} (W_{kk}(t') - W_{km}(t')) y_{km}^* = \\ & -P_{l_k}(t') - jQ_{l_k}(t'), k \notin \mathcal{G}, \end{aligned} \quad (14d)$$

$$\underline{V}_k^2 \leq W_{kk}(t') \leq \bar{V}_k^2, \quad k \in \mathcal{N}, \quad (14e)$$

$$\Im(W_{km}(t')) \leq \Re(W_{km}(t')) \tan(\theta_{km}^{max}), (k, m) \in \mathcal{L}, \quad (14f)$$

$$W(t') \succeq 0, \quad (14g)$$

$$\text{rank}(W(t')) = 1, \quad (14h)$$

$$\sum_{t'=t}^{t_{k_n, d}} u_h \bar{P}_{k_n} \tau_{k_n}(t') \geq \mathcal{P}_{k_n}(t), \quad (14i)$$

$$\tau_{k_n}(t') \in \{0, 1\}, \quad (14j)$$

By now, the difficulty of (14) is concentrated on the multiple nonconvex matrix rank-one constraints (14g) and the massive integer constraints (14i) and (14j). A two-stage nonsmooth algorithm is proposed to efficiently handle the two main difficulties step by step.

In the first stage, the matrix rank-one constraints (14g) is relaxed, then we solve the following problem to locate the solution of charging binary variable  $\tau_{k_n}(t')$ ,

$$\min_{W(t'), R(t'), \tau_{k_n}(t')} F_{[t, \Psi(t)]} \quad \text{s.t. (14b) - (14g), (14i), (14j)}. \quad (15)$$

Suppose that  $(W^{(\kappa+1)}(t), R^{(\kappa+1)}(t))$  and  $\hat{\tau}_{k_n}(t)$  is the optimal solution of (15). If  $\text{rank}(\hat{W}(t)) \equiv 1$ ,  $t' \in [t, \Psi(t)]$ , then  $\hat{V}(t')$  such that  $\hat{W}(t') = \hat{V}(t') \hat{V}^H(t')$  together with  $\hat{R}(t')$  and  $\hat{P}_{k_n}(t')$  constitute the optimal solution of the nonconvex optimization problem (13). Otherwise, we go to the next stage.

In the second stage by substituting  $\hat{\tau}_{k_n}(t')$  into (14c), we solve the following problem to obtain the solution of  $W(t')$  and  $R(t')$ ,

$$\min_{W(t'), R(t')} F(P_g(t')) := \sum_{t'=t}^{\Psi(t)} \sum_{k \in \mathcal{G}} f(P_{g_k}(t')), \quad \text{s.t. (14d) - (14h)}, \quad (16a)$$

$$\begin{aligned} & \sum_{m \in \mathcal{N}(k)} (W_{kk}(t') - W_{km}(t')) y_{km}^* = (P_{g_k}(t') - P_{l_k}(t')) \\ & - \sum_{k_n \in \mathcal{C}(t)} \bar{P}_{k_n} \hat{\tau}_{k_n}(t') + j(Q_{g_k}(t') - Q_{l_k}(t')), \quad k \in \mathcal{G}, \end{aligned} \quad (16b)$$

Following is the specific procedure to solve the two stages problem (15) and (16).

#### A. The first stage: iterative procedure to solve (15)

From (14i) we can find an integer number  $0 < \bar{\tau}_{k_n} < t_{k_n,d} - t_{k_n,a}$  such that

$$\sum_{t=t_{k_n,a}}^{t_{k_n,b}} \tau_{k_n}(t) = \bar{\tau}_{k_n} := \lceil \frac{C_{k_n}(1 - S_{k_n}^0)}{u_h \bar{P}_{k_n}} \rceil, \quad (17)$$

where  $\lceil x \rceil$  is the smallest integer that is not less than  $x$ . The discrete constraints (14i) and (14j) are equivalent to the following set of continuous constraints

$$(17), \quad \tau_{k_n}(t) \in [0, 1], \quad t \in [t_{k_n,a}, t_{k_n,b}], \quad (18)$$

$$g(\tau) = \sum_{t=t_{k_n,a}}^{t_{k_n,b}} \sum_{k_n \in \mathcal{C}(t)} \tau_{k_n} \geq \bar{\tau} := \sum_{k_n \in \mathcal{C}(t)} \bar{\tau}_{k_n} \quad (19)$$

for any  $L > 1$  (generally  $L$  is set as 1.5). The difficulty is now concentrated on the reverse convex constraint (19). We then address (15) by

$$\min_{W(t'), R(t'), \tau_{k_n}(t')} F_{[t, \Psi(t)]} + \mu_1 \left( \frac{1}{g(\tau)} - \frac{1}{\bar{\tau}} \right) \quad (20a)$$

$$\text{s.t.} \quad (14b) - (14g), \quad (18), \quad (19), \quad (20b)$$

where  $\mu_1 > 0$  is a penalty parameter.

At each iteration  $\kappa$ , we solve

$$\min_{W(t'), R(t'), \tau_{k_n}(t')} F_{[t, \Psi(t)]} + \mu_1 \left( \frac{1}{g^{(\kappa)}(\tau)} - \frac{1}{\bar{\tau}} \right) \quad (21a)$$

$$\text{s.t.} \quad (20b), \quad L\tau_{k_n}(t) \geq (L-1)\tau_{k_n}^{(\kappa)}(t), \quad (21b)$$

where  $g^{(\kappa)}$  is the linearization of  $g$  based on the first order Taylor expansion at  $\tau^{(\kappa)}$ :

$$g^{(\kappa)}(\tau) = L \sum_{t=t_{k_n,a}}^{t_{k_n,b}} \sum_{k_n \in \mathcal{C}(t)} (\tau_{k_n}^{(\kappa)}(t))^{L-1} \tau_{k_n}(t) - (L-1) \sum_{t=t_{k_n,a}}^{t_{k_n,b}} \sum_{k_n \in \mathcal{C}(t)} (\tau_{k_n}^{(\kappa)}(t))^L. \quad (22)$$

An initial point  $\tau_{k_n}^{(0)}$  can be obtained by relaxing constraints (14h) and (14j) and solve the semi-definite relaxation (SDR):

$$\min_{W(t'), R(t'), \tau_{k_n}(t')} F_{[t, \Psi(t)]} \quad \text{s.t. (14b) - (14g), (14i)}. \quad (23)$$

The above iterative procedure terminates at  $\frac{1}{g^{(\kappa)}(\tau)} - \frac{1}{\bar{\tau}} < \epsilon$ .

### B. The second stage: iterative procedure to solve (16)

In optimization (16), it should be noted that at each time  $t$ , constraint (14h) is involved with  $\Psi(t) - t$  nonconvex matrix rank-one constraints. However, in the dynamic charging problem only the current state and control will be updated. Thus, (16) can be simplified by,

$$\min_{W(t'), R(t')} F(P_g(t')) := \sum_{t'=t}^{\Psi(t)} \sum_{k \in \mathcal{G}} f(P_{g_k}(t')), \quad (24a)$$

$$\text{s.t. (14d) - (14g), (16b), } t' \in [t, \Psi(t)], \quad (24b)$$

$$\text{rank}(W(t)) = 1, \quad (24c)$$

with only one matrix rank-one constraint (24c).

Following our previous works [14], [19]–[22], optimization (24) can be solved very efficiently by a nonsmooth optimization algorithm (NOA), which is to proposed to deal with the matrix rank-one constraint (24c). Optimization (24) is equivalent to

$$\min_{W(t'), R(t')} F_{\mu}(W(t'), P_g(t')) := F(P_g(t')) + \mu_2(\text{Trace}(W(t')) - \lambda_{\max}(W(t'))), \quad (25a)$$

$$\text{s.t. (14d) - (14g), (16b), } t' \in [t, \Psi(t)], \quad (25b)$$

which can be solved by the following iterative procedure:

$$\begin{aligned} \min_{W(t'), R(t')} F_{\mu}^{(\kappa)}(W(t'), R(t')) &:= F(P_g(t')) + \mu_2(\text{Trace}(W(t'))) \\ &- (w_{\max}^{(\kappa)}(t'))^H W(t') w_{\max}^{(\kappa)}(t') \quad \text{s.t. (14d) - (14g), (16b), } t' \in [t, \Psi(t)], \end{aligned} \quad (26)$$

where  $w_{\max}^{(\kappa)}(t)$  denotes the normalized eigenvector corresponding to the eigenvalue  $\lambda_{\max}(W^{(\kappa)}(t))$ ,  $\mu_2 > 0$  is a penalty parameter. The reader is also referred to [14] for the convergence proof of the above procedure (26). The above procedure terminates at  $0 \leq \text{Trace}(W^{(\kappa)}(t)) - \lambda_{\max}(W^{(\kappa)}(t)) \leq \text{Trace}(W^{(\kappa)}(t)) - (w_{\max}^{(\kappa)}(t))^H W^{(\kappa)}(t) w_{\max}^{(\kappa)}(t) \leq \epsilon$ .

---

**Algorithm 1** Two-stage nonsmooth optimization algorithm for dynamic scheduling (14)

---

- 1: **Set**  $\kappa = 0$  solve (24) to obtain the initial point of  $\tau_{k_n}^{(0)}$ ,
  - 2: **Until**  $\frac{1}{g^{(\kappa)}(\tau)} - \frac{1}{\bar{\tau}} < \epsilon$ , **solve** (21) to find the optimal solution of  $(W^{(\kappa+1)}(t'), R^{(\kappa+1)}(t'), \tau_{k_n}^{(\kappa+1)}(t'))$  and **reset**  $\kappa + 1 \rightarrow \kappa$ ,
  - 3: **if**  $\text{rank}(\hat{W}(t')) \equiv 1$ ,  $t' \in [t, \Psi(t)]$  **then** accept  $(W^{(\kappa)}(t'), R^{(\kappa)}(t'), \tau_{k_n}^{(\kappa+1)}(t'))$  as the optimal solution of the nonconvex optimization problem (14),
  - 4: **else** set  $\kappa = 0$ ,  $\hat{\tau}_{k_n}(t) = \tau_{k_n}^{(\kappa)}(t')$  **Until**  $\text{Trace}(W^{(\kappa)}(t)) - (w_{\max}^{(\kappa)}(t))^H W^{(\kappa)}(t) w_{\max}^{(\kappa)}(t) \leq \epsilon$ , **solve** (26) to find the optimal solution  $(W^{(\kappa+1)}(t'), R^{(\kappa+1)}(t'))$  and **reset**  $\kappa + 1 \rightarrow \kappa$ ,
  - 5: **end if**
  - 6: **Accept**  $(W^{(\kappa)}(t'), R^{(\kappa)}(t'), \tau_{k_n}^{(\kappa)}(t'))$  as the optimal solution of the dynamic scheduling problem (14).
- 

In summary, our proposed MPC-based computation for (11) is based on two-stage iterative procedure solving (15) for online coordinating PEV charge  $\hat{\tau}_{k_n}(t)$  and solving (16) for online updating the generated voltage  $\hat{V}(t)$  for the generated power  $\hat{R}(t)$  by

$$\hat{V}(t) = \sqrt{\lambda_{\max}(W^{(\kappa)})} w_{\max}^{(\kappa)}(t), \quad (27)$$

whenever the solution  $\hat{W}(t)$  of SDR (16) is not of rank-one. If  $\text{rank}(\hat{W}(t)) = 1$ , it is obvious that  $\hat{V}(t) = \sqrt{\lambda_{\max}(\hat{W}(t))} \hat{w}_{\max}(t)$  with the normalized eigenvector  $\hat{w}_{\max}(t)$  corresponding to  $\lambda_{\max}(\hat{W}(t))$  is the optimal solution of (13), which is what we need. Algorithm (NOA) 1 is the pseudo-code for the above two-stage dynamic scheduling optimization.

## V. SIMULATION RESULTS

### A. Simulation setup

The SDPs (24), (21) (26) and (25) are computed using Sedumi [23] interfaced by CVX [24] on a Core i5-3470 processor. Four power networks from Matpower [25] are chosen. The tolerance  $\epsilon = 10^{-4}$  is set for the stop criterions.

Generally, PEVs are charged after their owners' working hours. We focus on the charging period from 6:00 pm to 6:00 am of the next day, which is then uniformly divided into 24 time slots of 30 minute length [2]. Accordingly, the charging time horizon is  $\mathcal{T} = \{1, 2, \dots, 24\}$ . It is also reasonable to assume that the PEVs arrive during the time period from 6:00 pm to

midnight. The PEVs must be fully charged after being plugged into the grid. The arrival times of PEVs are assumed to be independent and are generated by a truncated normal distribution  $(20, 1.5^2)$ , which is depicted by Fig. 2.

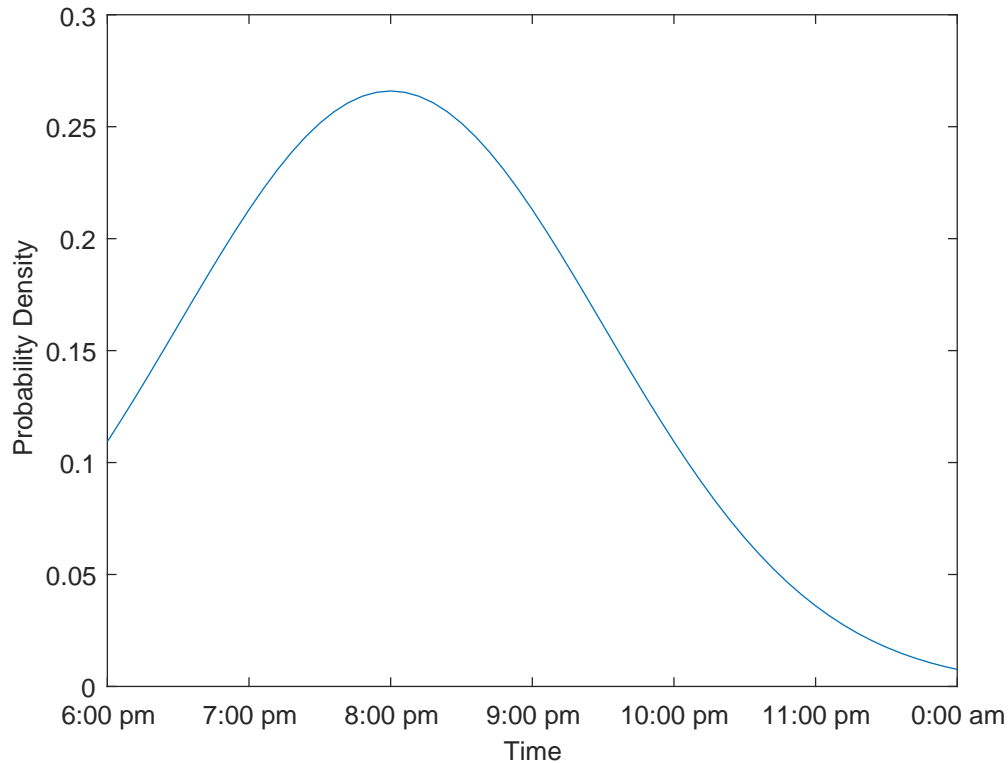


Fig. 2: The probability density of PEVs' arrivals

We assume that the PEVs are Tesla Model S's, which have a battery capacity of 100 KWh [26]. The SOC of all PEVs is set as 20%. The structure and physical limits of the considered grids are given in the Matpower library [25] together with the specific cost functions  $f(P_{g_k}(t))$ .

Without loss of generality, PEV loads are connected at the generator buses, which means each generator bus will serve as a charging station.

The price-inelastic load  $P_{l_k}(t)$  is calculated as

$$P_{l_k}(t) = \frac{l(t) \times \bar{P}_{l_k} \times T}{\sum_{t=1}^{24} l(t)}, \quad t \in \mathcal{T}, \quad (28)$$

where  $\bar{P}_{l_k}$  is the load demand specified by [25] and  $l(t)$  is the residential load demand taken from [27]. Four profiles are taken from different days in 2017. Profile 1 is the residential load and energy price from 6:00 pm on 7th May to 6:00 am on 8th May, Profile 2 is from 6:00 pm on 7th June to 6:00 am on 8th June, Profile 3 is from 6:00 pm on 7th July to 6:00 am on 8th

July, and Profile 4 is from 6:00 pm on 7th August to 6:00 am on 8th August. Fig. 3 and Fig. 4 provide the residential load demand and energy price for these profiles.

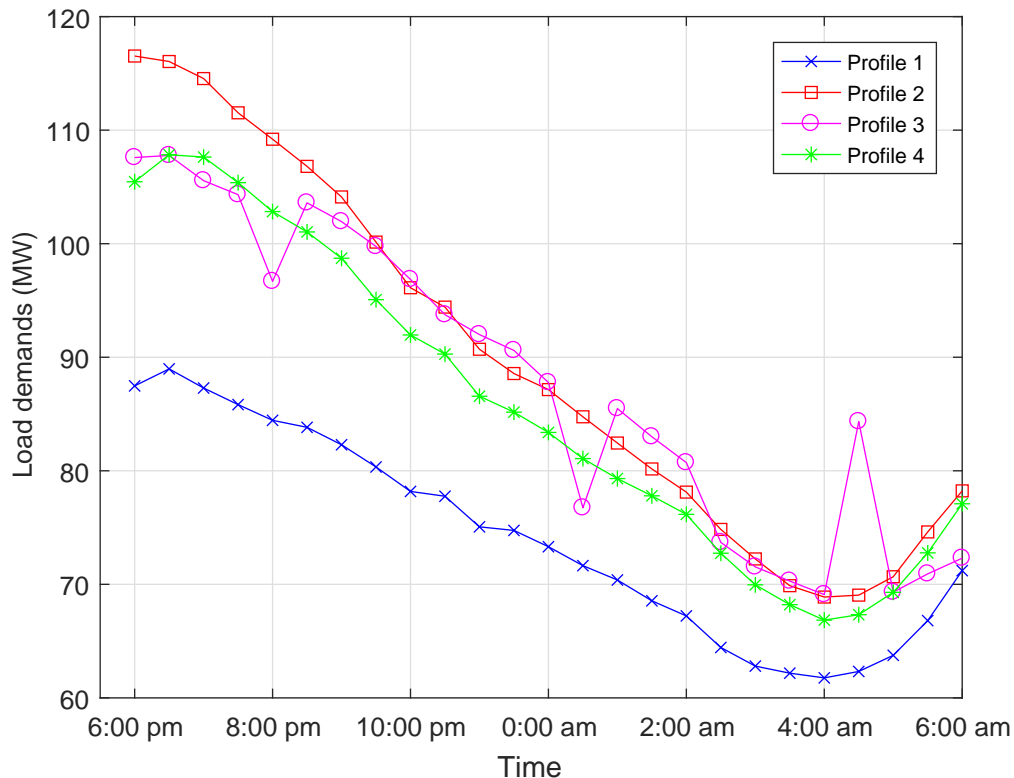


Fig. 3: Residential load demands of four profiles

### B. MPC-based dynamic scheduling computational results

1) *Four network simulation:* We test MPC-based online computation for Case9, Case14, Case30 and Case57 from [25] and profile 2 of the residential data. The information on these networks is given in Table. I, where the first column is the name of network, the second column indicates the numbers of buses, generators and branches. The dimension of  $W(t)$  is given in the third column, while the total number of PEVs is shown in the last column. The computational results are summarized in Table II. Again, the first column is the network name. The second column presents the number of binary variables  $\tau_{k_n}(t')$  in (13). The value of the penalty parameter  $\mu_1$  in (21) and  $\mu_2$  in (26) are given in the third column and fourth column, respectively. The computational value of the first stage and the second stage are respectively provided in the fifth column and sixth column. In the last column, the average running time is presented.

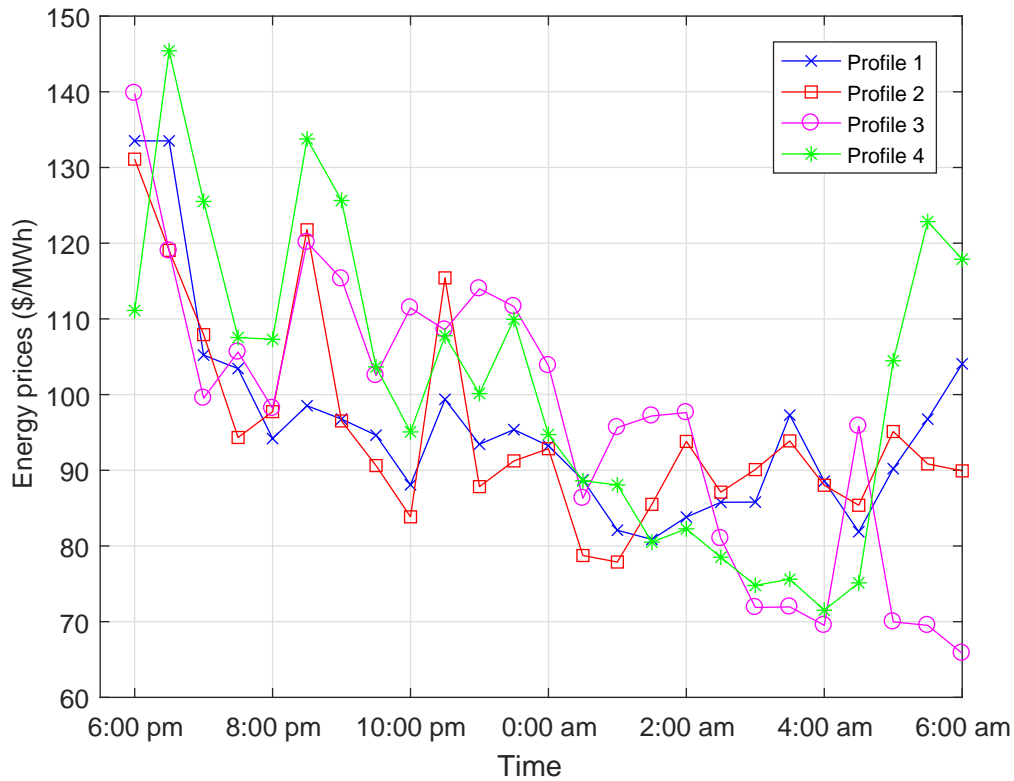


Fig. 4: Energy prices for four profiles

TABLE I: Information on four networks

	Buses/Generators/Branches	Dim. of $W(t)$	PEVs
Case9	9/3/9	$\mathbb{C}^{9 \times 9}$	126
Case14	14/5/20	$\mathbb{C}^{14 \times 14}$	210
Case30	30/6/24	$\mathbb{C}^{30 \times 30}$	252
Case57	57/7/80	$\mathbb{C}^{57 \times 57}$	294

2) *Four residential profile simulation:* We consider Case30 together with four different residential profiles. The computational results are provided in Table III, whose format is similar to Table II.

## VI. CONCLUSIONS

Joint PEV charging scheduling and power control for power grids to serve both PEVs at a competitive cost and residential power demands at a competitive operating cost is very difficult due to the random nature of PEVs' arrivals and demands. We have proposed a novel and easily-

TABLE II: MPC-based two-stage results

	Binary variables	$\mu_1$	$\mu_2$	Stage-1	Stage-2	Time(s)
Case9	1512	1	10	23854.7	23858.3	25.5
Case14	2520	1	-	53431.1	53431.1	18.5
Case30	3012	1	10	5634.9	5639.6	35.5
Case57	3528	10	10	87490.7	87502.7	89.7

TABLE III: MPC results for Case30 with four different residential profiles

	Binary variables	$\mu_1$	$\mu_2$	Stage-1	Stage-2	Time(s)
Profile 1	3012	1	10	7834.5	7836.7	34.8
Profile 2	3012	1	10	5634.9	5639.6	35.5
Profile 3	3012	1	10	8632.5	8636.4	36.7
Profile 4	3012	1	10	6541.3	6545.1	35.2

implemented MPC-based two-stage computational algorithm that can achieve a globally optimal solution.

## REFERENCES

- [1] N. Rotering and M. Ilic, "Optimal charge control of plug-in hybrid electric vehicles in deregulated electricity markets," *IEEE Trans. Power Systems*, vol. 26, pp. 1021–1029, Aug 2011.
- [2] C. Jin, J. Tang, and P. Ghosh, "Optimizing electric vehicle charging: A customer's perspective," *IEEE Trans. Veh. Tech.*, vol. 62, pp. 2919–2927, Sept 2013.
- [3] E. Sortomme, M. M. Hindi, S. J. MacPherson, and S. Venkata, "Coordinated charging of plug-in hybrid electric vehicles to minimize distribution system losses," *IEEE transactions on smart grid*, vol. 2, no. 1, pp. 198–205, 2011.
- [4] S. Huang, H. Safiullah, J. Xiao, B.-M. S. Hodge, R. Hoffman, J. Soller, D. Jones, D. Dinninger, W. E. Tyner, A. Liu, *et al.*, "The effects of electric vehicles on residential households in the city of indianapolis," *Energy Policy*, vol. 49, pp. 442–455, 2012.
- [5] E. Sortomme and M. A. El-Sharkawi, "Optimal charging strategies for unidirectional vehicle-to-grid," *IEEE Trans. Smart Grid*, vol. 2, no. 1, pp. 131–138, 2011.
- [6] J. F. Franco, M. J. Rider, and R. Romero, "A mixed-integer linear programming model for the electric vehicle charging coordination problem in unbalanced electrical distribution systems," *IEEE Trans. Smart Grid*, vol. 6, no. 5, pp. 2200–2210, 2015.
- [7] C. S. Antnez, J. F. Franco, M. J. Rider, and R. Romero, "A new methodology for the optimal charging coordination of electric vehicles considering vehicle-to-grid technology," *IEEE Trans. Sustainable Energy*, vol. 7, pp. 596–607, April 2016.
- [8] H. Xing, M. Fu, Z. Lin, and Y. Mou, "Decentralized optimal scheduling for charging and discharging of plug-in electric vehicles in smart grids," *IEEE Trans. Power Syst.*, vol. 31, no. 5, pp. 4118–4127, 2016.
- [9] L. Hua, J. Wang, and C. Zhou, "Adaptive electric vehicle charging coordination on distribution network," *IEEE Trans. Smart Grid*, vol. 5, no. 6, pp. 2666–2675, 2014.

- [10] K. Clement-Nyns, E. Haesen, and J. Driesen, "The impact of vehicle-to-grid on the distribution grid," *Electric Power Systems Research*, vol. 81, no. 1, pp. 185–192, 2011.
- [11] W. Tang and Y. J. A. Zhang, "A model predictive control approach for low-complexity electric vehicle charging scheduling: optimality and scalability," *IEEE Trans. Power Systems*, vol. 32, no. 2, pp. 1050–1063, 2017.
- [12] P. Malysz, S. Sirouspour, and A. Emadi, "An optimal energy storage control strategy for grid-connected microgrids," *IEEE Trans. Smart Grid*, vol. 5, no. 4, pp. 1785–1796, 2014.
- [13] A. Ravichandran, S. Sirouspour, P. Malysz, and A. Emadi, "A chance-constraints-based control strategy for microgrids with energy storage and integrated electric vehicles," *IEEE Trans. Smart Grid*, 2016.
- [14] Y. Shi, H. D. Tuan, H. Tuy, and S. Su, "Global optimization for optimal power flow over transmission networks," *J. Global Optimz. (to appear)*, 2017.
- [15] J. W. Polderman and J. C. Willems, *Introduction to Mathematical Systems Theory: A Behavioral Approach, 2nd Edition*. Springer-Verlag New York, 1998.
- [16] E. F. Camacho and C. Bordons, *Model Predictive Control*. Springer: Springer-Verlag, 2004.
- [17] A. Mesbah, "Stochastic model predictive control: An overview and perspectives for future research," *IEEE Control Systems Mag.*, vol. 36, no. 6, pp. 30–44, 2016.
- [18] H. D. Tuan, A. Savkin, T. Nguyen, and H. T. Nguyen, "Decentralised model predictive control with stability constraints and its application in process control," *J. of Process Control*, vol. 26, pp. 73–89, 2015.
- [19] A. H. Phan, H. D. Tuan, H. H. Kha, and D. T. Ngo, "Nonsmooth optimization for efficient beamforming in cognitive radio multicast transmission," *IEEE Trans. Sign. Process.*, vol. 60, no. 6, pp. 2941–2951, 2012.
- [20] Y. Shi, H. D. Tuan, S. W. Su, and H. H. M. Tam, "Nonsmooth optimization for optimal power flow over transmission networks," in *2015 IEEE Global Conf. Signal Info. Process. (GlobalSIP)*, pp. 1141–1144, Dec. 2015.
- [21] A. A. Nasir, H. D. Tuan, D. T. Ngo, T. Q. Duong, and H. V. Poor, "Beamforming design for wireless information and power transfer systems: Receive power-splitting versus transmit time-switching," *IEEE Trans. Commun.*, vol. 65, no. 2, pp. 876–889, 2017.
- [22] Y. Shi, H. D. Tuan, and P. Apkarian, "Nonconvex spectral optimization algorithms for reduced-order  $\mathcal{H}_\infty$ -LPV-LFT controllers," *Int. J. Nonlinear Robust Control*, vol. 27, 2017.
- [23] J. Sturm, "Using SeDuMi 1.02, a MATLAB toolbox for optimization over symmetric cones," *Optimization Methods and Software*, vol. 11–12, pp. 625–653, 1999.
- [24] M. Grant and S. Boyd, "CVX: Matlab software for disciplined convex programming, version 2.1." <http://cvxr.com/cvx>, Mar. 2014.
- [25] R. D. Zimmerman, C. E. Murillo-Sanchez, and R. J. Thomas, "Matpower: Steady-state operations, planning, and analysis tools for power systems research and education," *IEEE Trans. Power Systems*, vol. 26, pp. 12–19, Feb 2011.
- [26] "Tesla model s." [https://en.wikipedia.org/wiki/Tesla\\_Model\\_S](https://en.wikipedia.org/wiki/Tesla_Model_S). Accessed: 2017-06-06.
- [27] "Australian energy market operator." <https://www.aemo.com.au/Electricity/National-Electricity-Market-NEM/Data-dashboard#price-demand>. Accessed: 2017-06-06.